PERGAMON

Journal of Atmospheric and Solar-Terrestrial Physics 62 (2000) 467–475

Journal of ATMOSPHERIC AND SOLAR-TERRESTRIAL PHYSICS

Transverse ion acceleration mechanisms in the aurora at solar minimum: occurrence distributions

E.J. Lund[a,*], E. Möbius[a,b], C.W. Carlson[c], R.E. Ergun[c], L.M. Kistler[a,b], B. Klecker[d], D.M. Klumpar[e], J.P. McFadden[c], M.A. Popecki[a], R.J. Strangeway[f], Y.K. Tung[c]

[a]*Space Science Center, University of New Hampshire, Durham, NH 03824-3525, USA*
[b]*Physics Department, University of New Hampshire, Durham, NH 03824-3525, USA*
[c]*Space Sciences Laboratory, University of California, Berkeley, CA, USA*
[d]*Max-Planck-Institut für extraterrestrische Physik, Garching, Germany*
[e]*Lockheed Martin Advanced Technology Center, Palo Alto, CA, USA*
[f]*Institute for Geophysics and Planetary Physics, University of California, Los Angeles, CA, USA*

Received 15 June 1999; accepted 27 August 1999

Abstract

We present a statistical study of 714 ion conic events detected by the Fast Auroral Snapshot Explorer (FAST) from September 1996 to February 1997. Ninety-nine percent of the events found are associated with either broadband extremely low frequency (BBELF) emissions or electromagnetic ion cyclotron (EMIC) waves. Lower hybrid waves are much less important in transverse ion acceleration above 2000 km. The BBELF events are more numerous, comprising some 84% of ion conic events identified, and occur at all local times, with a peak near noon and a minimum near dusk. The EMIC events are concentrated in the dusk to midnight sector and are more likely to occur at lower latitudes compared to the BBELF events. The occurrence rate of EMIC conics has an apparent local minimum at 2000–2500 km, while the BBELF conic occurrence rate varies only slowly between 2000 km and the FAST apogee of 4200 km. The occurrence rate of EMIC conics is more strongly correlated with K_p than the BBELF conic occurrence rate. These results are consistent with previous studies of ion conics at lower altitudes. The correlation of both BBELF and EMIC ion conics with phenomena that are associated with parallel electric fields suggests that parallel electric fields play a significant role in transverse ion heating in the aurora.

1. Introduction

In the years since Sharp et al. (1977) first deduced the existence of a mechanism that accelerates ions transversely to the magnetic field at auroral latitudes, ion conics have come to be recognized as a ubiquitous feature of the aurora. A large number of rocket (Whalen et al., 1978; Yau et al., 1983; Kintner et al., 1986; Lynch et al., 1996) and satellite (Gorney et al., 1981; Klumpar et al., 1984; Miyake et al., 1991, 1996; Knudsen et al., 1998a; André et al., 1998) studies have attempted to elucidate the mechanisms which produce transverse ion acceleration.

* Corresponding author. Tel.: +1-603-862-0758; fax: +1-603-862-0311.
E-mail address: eric.lund@unh.edu (E.J. Lund).

1364-6826/00/$ - see front matter
PII: S1364-6826(00)00013-4

In recent years, three types of wave emissions have been found in association with ion conics at altitudes below 2000 km. The most common is a broad-band extremely low frequency (BBELF) emission which is correlated with field-aligned suprathermal electron bursts in the downward current region (Knudsen et al., 1998a and references therein). The wave mode or modes which produce these emissions have not been conclusively identified; suggested candidates include inhomogeneous energy–density driven instability (Amatucci et al., 1998; Koepke et al., 1999), solitary kinetic Alfvén waves (Knudsen and Wahlund, 1998), ion acoustic waves (Wahlund et al., 1998), electron acoustic waves (Cattell et al., 1998), and electrostatic solitary waves (Ergun et al., 1998). There is evidence that BBELF emissions are often Alfvénic at the lowest frequencies and electrostatic near and above the oxygen gyrofrequency (Heppner et al., 1993; André et al., 1998). The other two types of wave emissions, electromagnetic ion cyclotron (EMIC) waves (Erlandson et al., 1994) and lower hybrid (LH) waves (Kintner et al., 1986), are associated with field-aligned electrons occurring within "inverted-V" structures. A recent statistical survey of the Freja data confirms that these three wave emissions account for nearly all of the ion conics seen near 1700 km (André et al., 1998).

When EMIC waves accompany an ion conic, He^+ is found to be energized more efficiently than other species (Lund et al., 1998), and O^+ is preferentially accelerated over H^+ (Erlandson et al., 1994; Vaivads et al., 1999). The He^+ ions are apparently accelerated by a cyclotron resonant interaction with the waves near the altitude where their frequency equals the helium gyrofrequency f_{cHe}. Such a preferential acceleration is needed to explain the observed He^+ fluxes in a large fraction of the ion conics studied by Collin et al. (1988). The X-type He^+ distributions seen in the equatorial magnetosphere result from a similar process (Anderson and Fuselier, 1994; Horne and Thorne, 1997), and this mechanism is similar to a mechanism that has been proposed to account for anomalously high ^3He abundances in impulsive solar flares (Temerin and Roth, 1992; Roth and Temerin, 1997).

In the next section we show examples of the data from the Fast Auroral Snapshot Explorer (FAST). We then a present a statistical study of ion conics identified during September 1996–February 1997 and discuss some implications of our results. The present study is intended to complement the André et al. (1998) study by extending their analysis to the bottom of the potential drop in the upward current region and to comparable altitudes in the return current region. A case study of passes in which transverse ion acceleration by both BBELF and EMIC waves occurs is presented elsewhere (Lund et al., 1999).

2. Examples of data

The FAST was launched on August 21, 1996, into a 4200×350 km orbit with 83° inclination. An overview of the mission is given by Carlson et al. (1998a). The FAST carries the Time-of-flight Energy Angle Mass Spectrograph (TEAMS), which simultaneously measures 3D distributions of H^+, He^{2+}, He^+, and O^+ at 0.001–12 keV and also provides a mass spectrum over the range 1–60 AMU/q (Möbius et al., 1998).

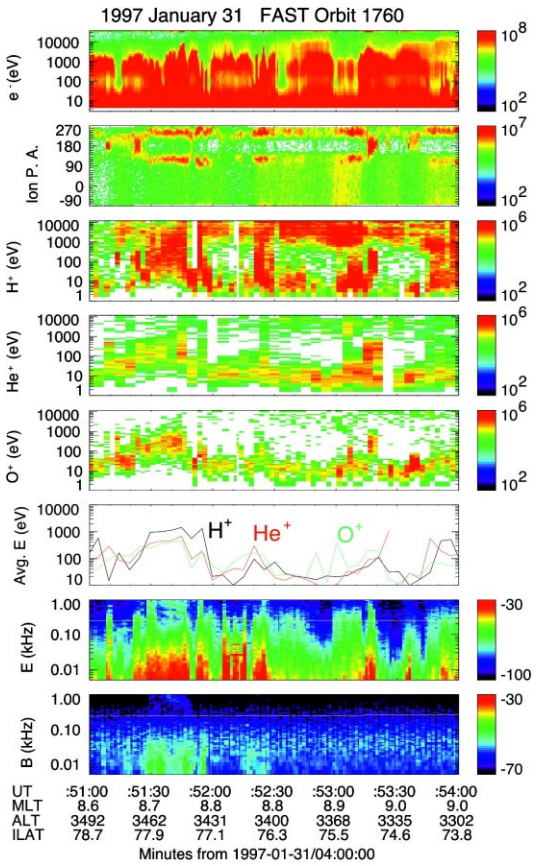

Fig. 1. Overview of the BBELF ion conic event from the dayside on orbit 1760. From top to bottom: electron energy spectrogram; ion pitch angle spectrogram (all species); energy spectrograms for H^+, He^+, and O^+; average energy (energy flux divided by number flux); and ELF electric and magnetic field frequency spectrograms. The z-axis units are eV/(cm^2 s sr eV) for the particle data, dB (V/m)^2/Hz for the electric field spectrogram, and dB (nT)^2/Hz at 1 kHz for the magnetic field spectrogram, which has been multiplied by f^2 to reduce the dynamic range needed to display the data.

As the statistical study described below shows, almost all of the ion conic events seen by FAST are associated with either BBELF emissions or EMIC waves. Many of these events are also associated with other wave modes, in particular LH waves and electrostatic ion cyclotron (EIC) waves, but the correlation between the occurrence of LH or EIC waves and ion conics is not as good on shorter time scales as the correlation between BBELF or EMIC waves and ion conics. Similar associations between waves and ion conics have been found at lower altitudes (André et al., 1998).

An example of transverse ion heating by BBELF waves is shown in Fig. 1, which shows 3 min of data from a pass through the aurora near 09 MLT during a period of moderate geomagnetic activity ($K_p = 3$). Although most of the BBELF emissions that occur on this pass are electrostatic, the emissions at 04:51:30–04:52:00, which coincide with the most intense ion heating, have a significant magnetic component at frequencies up to $f_{cO} \approx 15$ Hz. The electrons are highly field-aligned (not shown), as is typical of the return current region (Carlson et al., 1998b). The characteristic energies (the energy flux of each species divided by the number flux for that species) at 04:51:39 UT are 1140 eV for H^+, 442 eV for He^+, and 403 eV for O^+; the energy ranges of the ions in the conic are approximately 50–3000 eV for all three species. The characteristic energy of H^+ may be apparently enhanced by the presence of plasma sheet protons, which dominate the total flux. We have attempted to separate the plasma sheet population from the conic population by setting the upper energy limit of the flux integrations to the energy above 100 eV with the fewest total counts, but because the lower energy limit of the plasma sheet varies, the plasma sheet population is not easily separated from the conic by an automated procedure. Throughout the event, the ion conic energies are positively correlated with the intensity of the BBELF waves.

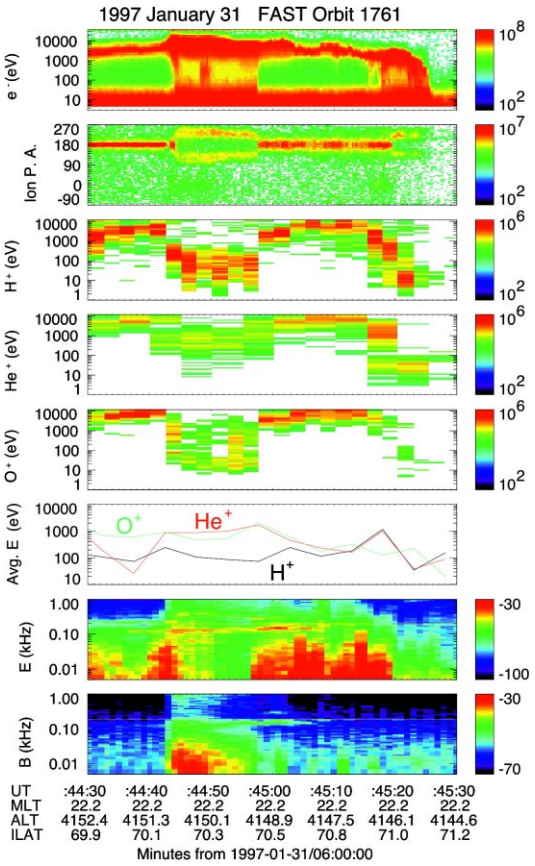

Fig. 2. Overview of the EMIC ion conic event from the nightside on orbit 1761. The format is the same as for Fig. 1.

Fig. 2 shows an example of transverse ion heating by EMIC waves. The data are taken from a pass near 22 MLT. This pass was geomagnetically quiet ($K_p = 1-$). The VLF portion of the wave spectrum shows evidence of a particularly low plasma density on this pass (Strangeway et al., 1998). The ion conic event occurs at 06:44:44–58, between two ion beams; many of the EMIC conics occur at the edge of an ion beam. The EMIC waves occur in the presence of secondary electrons, which are the leading candidate for generating the waves (Lund and LaBelle, 1997 and references therein). The characteristic energies at 06:44:52 are 1000 eV for He^+, 531 eV for O^+, and 86.2 eV for H^+. This ordering of energies is typical of EMIC ion conics. Note that while H^+ and O^+ have extended tails, He^+ is bulk heated.

3. Statistical results

For this paper we have examined 714 ion conic events which occurred between September 1996 and February 1997. Events were counted only if (1) the ion conic was clearly visible in H^+, He^+, and O^+ at the same time and (2) the spacecraft potential was within its output range (within approximately ± 50 V) during the event. The latter condition was imposed because severe spacecraft charging precludes electric field measurements at frequencies below ≈ 100 Hz. A maximum of one event of each type was counted on each inbound and each outbound pass through the auroral oval (a maximum of two BBELF and two EMIC events per hemisphere); where more than one event of a given type occurred on one pass, the event with the highest ion energies was used. For each event, the energy range covered by each ion in the conic was estimated by eye from the spectrogram, and the location, K_p index, and wave emissions were also recorded. For purposes of normalization, the total number of passes available at a given MLT, altitude, or K_p was obtained

from a database of crossings of 70° invariant latitude, which represents the average latitude of the auroral oval (the oval is equatorward of 70° on the nightside and poleward of 70° on the dayside), and a list of passes during which the TEAMS instrument was on and operating at the correct post-acceleration voltage for the lookup table in memory. The bin sizes used were 3 h in MLT, 2° in invariant latitude, 500 km in altitude, and nearest integer K_p. The orbital coverage by MLT and altitude is shown in Table 1.

The most common emission in our database is BBELF, which accounts for 601 of the events (84%). BBELF emissions are frequently seen in combination with VLF saucers (209 events) or lower hybrid emissions (237 events), but BBELF also occur alone (171 events) or with EIC waves (20 events). (These numbers include cases where more than one of the other three emissions is observed.) In all cases the BBELF emissions are best correlated with the ion heating. The various EMIC modes account for 106 of the events (15%) in our database. The proton cyclotron wave is observed in most of these events, either singly (90 events) or in combination with O^+ EMIC waves (13 events). Occasionally the He^+ cyclotron mode is seen (5 events, including 2 where the proton mode is not observed). Lower hybrid waves are also seen in 52 of these events.

Of the remaining events in our database, 6 are accompanied by LH waves, including one that is also associated with EIC waves. The last is associated with EIC waves and a saucer. The LH events include 4 of the 13 events at altitudes below 1600 km. In some of the LH events, the heating may actually be done by electrostatic BBELF waves, which do not propagate to the satellite altitude or by EMIC waves generated below the satellite altitude. In a detailed study of LH ion conics observed with Freja, Knudsen et al. (1998b) concluded that "the net effect [of LH cavitons] on the ambient ion populations is small" (p. 4248). Because the number of such events in our database is too small for meaningful statistics, we will not consider these events further in this paper.

The distribution of events in latitude and magnetic local time is shown in Fig. 3. We see that the BBELF conics (top) occur most frequently in the pre-noon sector, while EMIC conics (bottom) occur primarily in the pre-midnight sector. This point is illustrated in greater detail in Fig. 4, which shows normalized occurrence probabilities of BBELF and EMIC conics as a function of magnetic local time. EMIC conics are most common in the pre-midnight sector and rarely found near dawn; this distribution is consistent with the magnetic local time distribution that has been observed for EMIC waves alone (Saito et al., 1987; Erlandson and Zanetti, 1998). Fig. 4 also shows that the lack of BBELF events on the duskside is real and not merely the result of sampling bias. In fact, while BBELF events are about six times more numerous than EMIC events overall, in the 18–21 MLT sector the occurrence rate of EMIC conics is the same as for BBELF conics. The MLT distributions in Fig. 4 are qualitatively similar to the unnormalized distributions shown in Fig. 16 of André et al. (1998).

Fig. 5 shows the distribution of ion conic events with altitude. The distribution of BBELF events is steady above 2000 km; the portion of the distribution at lower altitudes is dominated by samples near dawn (03–09 MLT), which comprise 346 of the 373 available passes. We attempt to separate altitude and MLT effects in the BBELF occurrence rate in Table 2. Here we find that the altitude dependence changes with local time: the occurrence rate of BBELF heating rises with altitude near dawn, falls with altitude in the noon and dusk sectors, and is steady (within statistical uncertainties) near midnight. A more complete sample at lower altitudes would likely flatten the distribution in Fig. 5; such an altitude profile is consistent with the result of Miyake et al. (1996) that continuous heating up to at least 10,000 km is necessary to

Table 1
Available passes by altitude and magnetic local time

Altitude (km)	00–03	03–06	06–09	09–12	12–15	15–18	18–21	21–24	Total
≥ 4000	117	0	34	90	116	0	76	233	666
3500–4000	105	10	74	104	81	29	76	179	658
3000–3500	55	50	75	55	40	52	66	78	471
2500–3000	29	80	81	21	25	52	36	32	356
2000–2500	10	123	92	16	10	46	5	2	304
1500–2000	6	98	131	0	0	10	0	0	245
1000–1500	2	29	81	0	0	0	0	0	112
500–1000	0	0	6	4	2	0	1	0	13
< 500	0	0	1	0	0	0	0	2	3
Total	324	390	575	290	274	189	260	526	2828

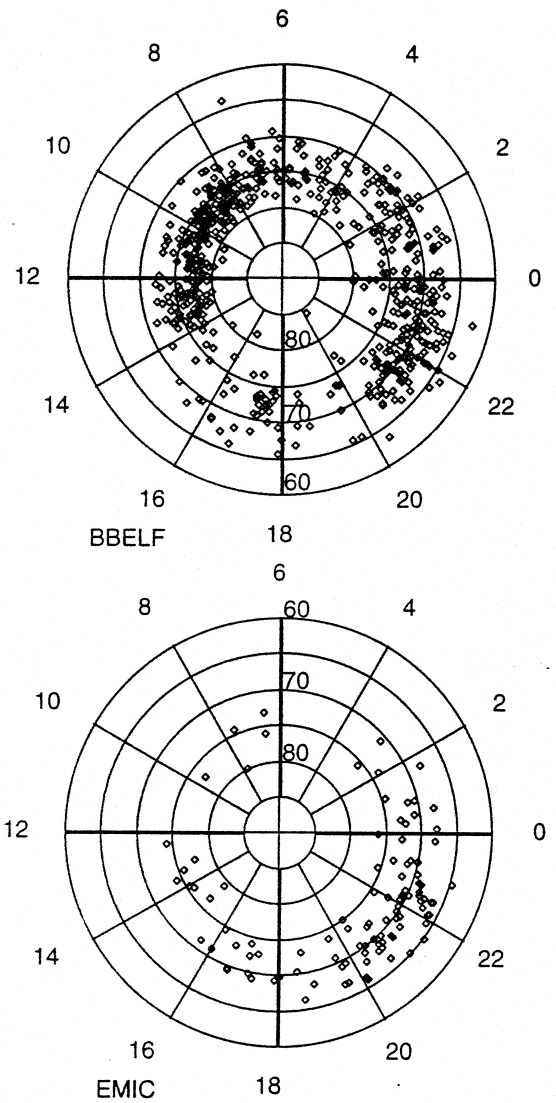

Fig. 3. Distribution of ion conic events in this study over invariant latitude and magnetic local time: (top) BBELF events, and (bottom) EMIC events.

account for the observed cone angles in ion conic distributions. The altitude distribution of our EMIC events has a local minimum just above 2000 km. This altitude distribution differs somewhat from the distribution of EMIC waves reported by Saito et al. (1987), which peaks below 2000 km and continues to decline at higher altitudes. This discrepancy may be due to the over-representation of the pre-midnight sector, where EMIC such on occurrence is highest, among our high altitude samples and the lack of available passes at 1000–2000 km in this local time sector.

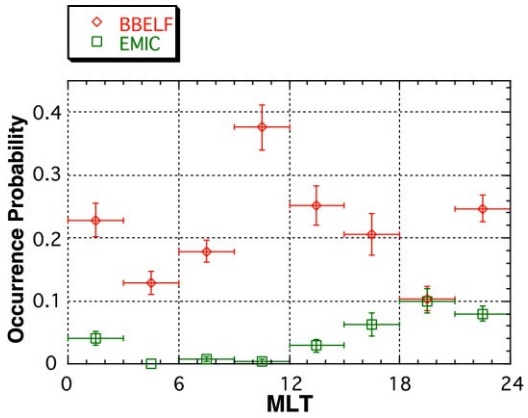

Fig. 4. Normalized occurrence probabilities of BBELF (red) and EMIC (green) ion conics as a function of magnetic local time. The error bars represent bin width in the horizontal direction and Poisson statistical errors in the vertical direction.

Fig. 6 shows the distribution of both types of ion conics with K_p. The trend towards a higher occurrence rate of EMIC conics as K_p increases from 0 to 4, agrees with the conclusion of Saito et al. (1987) that EMIC waves are more prevalent at higher K_p. The occurrence probability of BBELF events rises much more slowly with K_p. This result is consistent with an earlier study of DE 1 data (Yau et al., 1985), which found that the probability of intense upflowing ion events depended much more strongly on solar activity as measured by the $F_{10.7}$ radio flux than on K_p.

The BBELF ion conic events tend to occur at higher invariant latitudes (an average of 73.5°) than the EMIC events (an average of 70.7°), as expected from the differing local time distributions. As Fig. 7 shows,

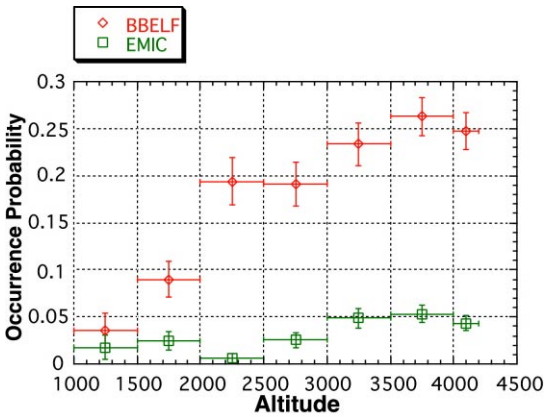

Fig. 5. Normalized occurrence probabilities of BBELF (red) and EMIC (green) ion conics as a function of altitude. The error bars have the same meaning as in Fig. 4.

Table 2
Occurrence probabilities of BBELF conics by altitude and magnetic local time

Altitude (km)	03–09	09–15	15–21	21–03
≥4000	0.471 ± 0.118	0.306 ± 0.039	0.079 ± 0.032	0.229 ± 0.026
3000–4000	0.330 ± 0.040	0.264 ± 0.031	0.130 ± 0.024	0.266 ± 0.025
2000–3000	0.125 ± 0.018	0.500 ± 0.083	0.223 ± 0.040	0.178 ± 0.049
< 2000	0.061 ± 0.013	0.833 ± 0.167	No events	No events

the distribution of BBELF events during active times ($K_p \geq 4-$) is shifted about 2° equatorward from the distribution of BBELF events during quiet times ($K_p \leq 1+$). This shift is consistent with expansion of the auroral oval during periods of enhanced geomagnetic activity.

That BBELF waves and EMIC waves have different effects on the ambient ions is shown in Fig. 8, which shows the ratios of maximum energies E_{He}/E_H (top) and E_{He}/E_O (bottom) for the two wave modes as histograms. The bar heights are normalized to the total number of events of each type. About 95% of the ion conics with BBELF waves have $0.4 < E_{He}/E_H < 2.5$, and about 85% have $0.7 < E_{He}/E_H < 1.4$, whereas for the events with EMIC waves, the median value of E_{He}/E_H is about 5. The distributions for E_{He}/E_O and E_O/E_H (not shown) show less drastic but qualitatively similar trends. These results show that the EMIC waves, which are narrow-banded, select the He^+ ions, presumably by a cyclotron resonant interaction, while BBELF waves have similar effects on all ion species. The lack of mass dependence of the maximum observed energy for BBELF events is consistent with previous observations (Knudsen et al., 1994; Norqvist et al., 1996).

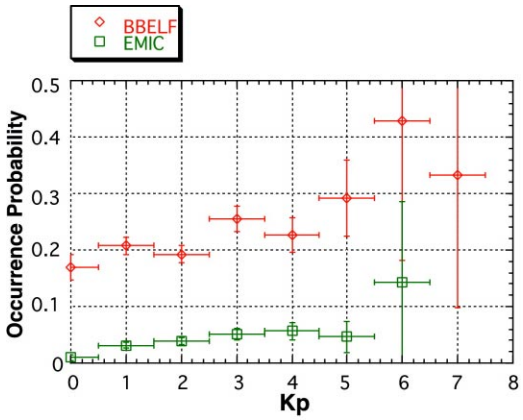

Fig. 6. Normalized occurrence probabilities of BBELF (red) and EMIC (green) ion conics as a function of K_p. The error bars have the same meaning as in Fig. 4.

4. Discussion

At one time lower hybrid waves were thought to be the waves responsible for most of the transverse ion heating in the auroral region (Kintner et al., 1986). However, we have found that the role of lower hybrid waves is essentially negligible at altitudes above 2000 km. There are two probable reasons for this discrepancy. One is an altitude effect: lower hybrid waves may produce core ion heating to a few eV at low altitudes, and BBELF and EMIC waves then heat the ions more strongly at higher altitudes; this scenario would explain why H^+ is heated at all in EMIC ion conics even though we have previously shown that protons show little or no response to EMIC waves (Lund et al., 1998). The other reason is a selection bias: most of the evidence for ion heating by lower hybrid waves comes from sounding rocket data, and almost all auroral sounding rockets are launched into active aurorae rather than under the quiet conditions which predominate at solar minimum. More recent sounding rocket observations (Lynch et al., 1996) do show that BBELF waves are more directly correlated with ion heating than lower hybrid waves.

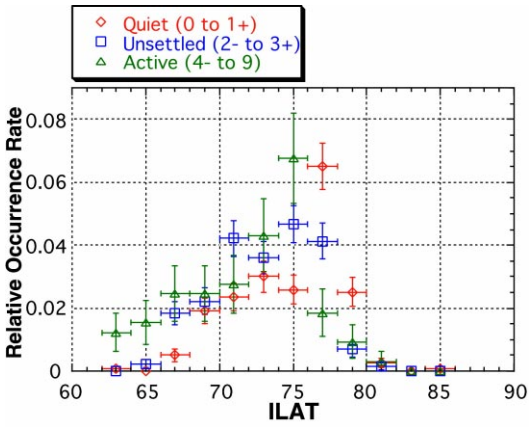

Fig. 7. Invariant latitude distribution of BBELF ion conics under quiet ($K_p \leq 1+$) (red), unsettled ($2- \leq K_p \leq 3+$) (blue), and active ($K_p \geq 4-$) (green) conditions. The error bars have the same meaning as in Fig. 4.

The MLT distribution of BBELF ion conics agrees well with the MLT distribution of ion conics associated with "electrostatic shocks" in the S3-3 data (Redsun et al., 1985). Since electrostatic shocks often imply parallel electric fields (Temerin et al., 1981), this result implies that BBELF ion conics are associated with parallel electric fields, as suggested by Gorney et al. (1985). A recent simulation of transverse proton heating by BBELF waves in the presence of a parallel electric field reproduced a typical observed ion conic distribution (Jasperse, 1998). We will investigate the role of parallel electric fields in BBELF ion conics in a future study.

The distribution of EMIC ion conics over MLT and invariant latitude is similar to that of ion beams (Gorney et al., 1981; Redsun et al., 1985). In fact, ion beams frequently occur at one or both edges of an EMIC ion conic. This association leads us to speculate that the change in altitude of the bottom of the potential drop with horizontal position may play a role in generating the EMIC waves; this conjecture could resolve the discrepancy noted by Lund and LaBelle (1997) (and references therein) that the growth rates of the traditionally assumed beam generation mechanism (Temerin and Lysak, 1984) are too low to account for the observed waves.

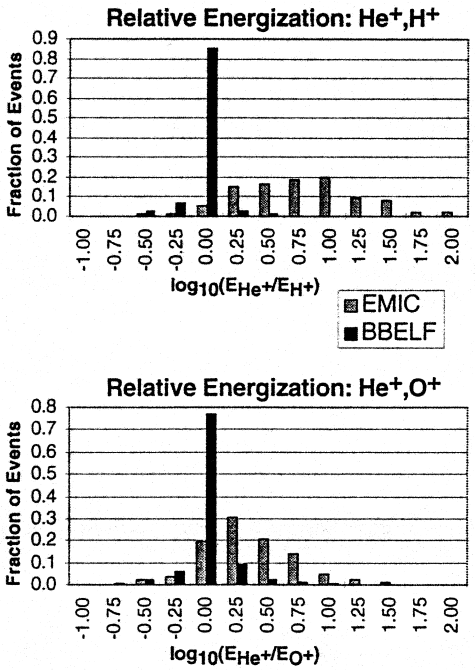

Fig. 8. Histogram of the ratio of maximum energies E_{He}/E_H (top) and E_{He}/E_O (bottom) for BBELF (black bars) and EMIC (gray bars) events. The histograms are normalized to the number of events of each type.

5. Conclusion

Our study has shown that 99% of ion conics at the altitudes sampled by FAST are associated with one of two types of emissions: BBELF emissions, which account for 84% of the events, and EMIC waves, which account for 15% of the events. Lower hybrid waves are nearly irrelevant in transverse ion acceleration above 2000 km. Our results generalize to higher altitudes the statistical results of André et al. (1998) at 1400–1750 km. The distribution of EMIC ion conics is similar to that of auroral EMIC waves alone (Saito et al., 1987). The similarity of our BBELF ion conic distribution to the distribution of "electrostatic shocks" associated with ion conics (Redsun et al., 1985) suggests that the parallel electric field in the return current region is a significant factor in BBELF ion conics.

Acknowledgements

The authors are indebted to the many unnamed individuals at UNH, MPE, LMATC, and UCB who contributed to the successful implementation of the TEAMS instrument. The authors would also like to thank W. Peria, G.T. Delory, and J. Loran for their efforts in producing and documenting data analysis software for the FAST AC fields. The work at the University of New Hampshire was supported by the National Aeronautics and Space Administration via a subcontract from the University of California at Berkeley under grant NAS5-31283.

References

Amatucci, W.E., Walker, D.N., Ganguli, G., Duncan, D., Antoniades, J.A., Bowles, J.H., Gavrishchaka, V., Koepke, M.E., 1998. Velocity-shear-driven ion cyclotron waves and associated transverse ion heating. Journal of Geophysical Research 103, 11711–11724.

Anderson, B.J., Fuselier, S.A., 1994. Response of thermal ions to electromagnetic ion cyclotron waves. Journal of Geophysical Research 99, 19413–19425.

André, M., Norqvist, P., Andersson, L., Eliasson, L., Eriksson, A.I., Blomberg, L., Erlandson, R.E., Waldemark, J., 1998. Ion energization mechanisms at 1700 km in the auroral region. Journal of Geophysical Research 103, 4199–4222.

Carlson, C.W., Pfaff, R.F., Watzin, J.G., 1998a. The fast auroral snapshot (FAST) mission. Geophysical Research Letters 25, 2013–2016.

Carlson, C.W., McFadden, J.P., Ergun, R.E., Temerin, M., Peria, W., Mozer, F.S., Klumpar, D.M., Shelley, E.G., Peterson, W.K., Moebius, E., Elphic, R., Strangeway, R., Cattell, C., Pfaff, R., 1998b. FAST observations in the downward auroral current region: energetic upgoing elec-

tron beams, parallel potential drops, and ion heating. Geophysical Research Letters 25, 2017–2020.

Cattell, C., Bergmann, R., Sigsbee, K., Carlson, C., Chaston, C., Ergun, R., McFadden, J., Mozer, F.S., Temerin, M., Strangeway, R., Elphic, R., Kistler, L., Moebius, E., Tang, L., Klumpar, D., Pfaff, R., 1998. The association of electrostatic ion waves, ion and electron beams and field-aligned currents: FAST observations of an auroral zone crossing near midnight. Geophysical Research Letters 25, 2053–2056.

Collin, H.L., Peterson, W.K., Drake, J.F., Yau, A.W., 1988. The helium components of energetic terrestrial ion upflows: their occurrence, morphology, and intensity. Journal of Geophysical Research 93, 7558–7564.

Ergun, R.E., Carlson, C.W., McFadden, J.P., Mozer, F.S., Delory, G.T., Peria, W., Chaston, C.C., Temerin, M., Roth, I., Muschietti, L., Elphic, R., Strangeway, R., Pfaff, R., Cattell, C.A., Klumpar, D., Shelley, E., Peterson, W., Moebius, E., Kistler, L., 1998. FAST observations of large-amplitude solitary structures. Geophysical Research Letters 25, 2041–2044.

Erlandson, R.E., Zanetti, L.J., Acuña, M.H., Eriksson, A.I., Eliasson, L., Boehm, M.H., Blomberg, L.G., 1994. Freja observations of electromagnetic ion cyclotron ELF waves and transverse oxygen ion acceleration on auroral field lines. Geophysical Research Letters 21, 1855–1858.

Erlandson, R.E., Zanetti, L.J., 1998. A statistical study of auroral electromagnetic ion cyclotron waves. Journal of Geophysical Research 103, 4627–4636.

Gorney, D.J., Clarke, A., Croley, D., Fennell, J., Luhmann, J., Mizera, P., 1981. The distribution of ion beams and conics below 8000 km. Journal of Geophysical Research 86, 83–89.

Gorney, D.J., Chiu, Y.T., Croley, D.R., 1985. Trapping of ion conics by downward parallel electric fields. Journal of Geophysical Research 90, 4205–4210.

Heppner, J.P., Liebrecht, M.C., Maynard, N.C., Pfaff, R.F., 1993. High-latitude distributions of plasma waves and spatial irregularities from DE 2 alternating current electric field observations. Journal of Geophysical Research 98, 1629–1652.

Horne, R.B., Thorne, R.M., 1997. Wave heating of He^+ by electromagnetic ion cyclotron waves in the magnetosphere: heating near the H^+–He^+ bi-ion resonance frequency. Journal of Geophysical Research 102, 11457–11471.

Jasperse, J.R., 1998. Ion heating, electron acceleration, and the self-consistent parallel E-field in downward auroral current regions. Geophysical Research Letters 25, 3485–3488.

Kintner, P.M., LaBelle, J., Scales, W., Yau, A.W., Whalen, B.A., 1986. Observations of plasma waves within regions of perpendicular ion acceleration. Geophysical Research Letters 13, 1113–1116.

Klumpar, D.M., Peterson, W.K., Shelley, E.G., 1984. Direct evidence for two-stage (bimodal) acceleration of ionospheric ions. Journal of Geophysical Research 89, 10779–10787.

Knudsen, D.J., Whalen, B.A., Abe, T., Yau, A., 1994. Temporal evolution and spatial dispersion of ion conics: evidence for a polar cusp heating wall. In: Burch, J.L., Waite, J.H. (Eds.), Solar System Plasmas in Space and Time, Geophysical Monograph, 84. American Geophysical Union, Washington, DC, pp. 163–169.

Knudsen, D.J., Wahlund, J.-E., 1998. Core ion flux bursts within solitary kinetic Alfvén waves. Journal of Geophysical Research 103, 4157–4169.

Knudsen, D.J., Clemmons, J.H., Wahlund, J.-E., 1998a. Correlation between core ion energization, suprathermal electron bursts, and broadband ELF plasma waves. Journal of Geophysical Research 103, 4171–4186.

Knudsen, D.J., Dovner, P.O., Eriksson, A.I., Lynch, K.A., 1998b. Effect of lower hybrid cavitons on core plasma observed by Freja. Journal of Geophysical Research 103, 4241–4249.

Koepke, M.E., Carroll, J.J., Zintl, M.W., 1999. Laboratory simulation of broadband ELF waves in the auroral ionosphere. Journal of Geophysical Research 104, 14397–14415.

Lund, E.J., LaBelle, J., 1997. On the generation and propagation of auroral electromagnetic ion cyclotron waves. Journal of Geophysical Research 102, 17241–17253.

Lund, E.J., Möbius, E., Tang, L., Kistler, L.M., Popecki, M.A., Klumpar, D.M., Peterson, W.K., Shelley, E.G., Klecker, B., Hovestadt, D., Temerin, M., Ergun, R.E., McFadden, J.P., Carlson, C.W., Mozer, F.S., Elphic, R.C., Strangeway, R.J., Cattell, C.A., Pfaff, R.F., 1998. FAST observations of preferentially accelerated He^+ in association with auroral electromagnetic ion cyclotron waves. Geophysical Research Letters 25, 2049–2052.

Lund, E.J., Möbius, E., Klumpar, D.M., Kistler, L.M., Pepeck, M.A., Klecker, B., Ergun, R.E., McFadden, J.P., Carlson, C.W., Strangeway, R.J., 1999. Direct comparison of transverse ion acceleration mechanisms in the aurora at solar minimum. Journal of Geophysical Research 104, 22801–22805.

Lynch, K.A., Arnoldy, R.L., Kintner, P.M., Bonnell, J., 1996. The AMICIST auroral sounding rocket: a comparison of transverse ion acceleration mechanisms. Geophysical Research Letters 23, 3293–3296.

Miyake, W., Mukai, T., Kaya, N., Fukunishi, H., 1991. EXOS-D observations of upflowing ion conics with high time resolution. Geophysical Research Letters 18, 341–344.

Miyake, W., Mukai, T., Kaya, N., 1996. On the origins of the upward shift of elevated (bimodal) ion conics in velocity space. Journal of Geophysical Research 101, 26961–26969.

Möbius, E., Kistler, L.M., Popecki, M.A., Crocker, K.N., Granoff, M., Jiang, Y., Sartori, E., Ye, V., Réme, H., Sauvaud, J.A., Cros, A., Aoustin, C., Camus, T., Médale, J.-L., Rouzaud, J., Carlson, C.W., McFadden, J.P., Curtis, D., Heetdirks, H., Croyle, J., Ingraham, C., Klecker, B., Hovestadt, D., Ertl, M., Eberl, F., Kästle, H., Künneth, E., Laeverenz, P., Seidenschwang, E., Shelley, E.G., Klumpar, D.M., Hertzberg, E., Parks, G.K., McCarthy, M., Korth, A., Rosenbauer, H., Gräve, B., Eliasson, L., Olsen, S., Balsiger, H., Schwab, U., Steinacher, M., 1998. The 3D plasma distribution function analyzers with time-of-flight mass discrimination for Cluster, FAST, and Equator-S. In: Pfaff, R.F., Borovsky, J.E., Young, D.T. (Eds.), Measurement Techniques in Space Plasmas: Particles, Geophysical Monograph, 102. American Geophysical Union, Washington, DC, pp. 243–248.

Norqvist, P., André, M., Eliasson, L., Eriksson, A.I.,

Blomberg, L., Lühr, H., Clemmons, J.H., 1996. Ion cyclotron heating in the dayside magnetosphere. Journal of Geophysical Research 101, 13179–13193.

Redsun, M.S., Temerin, M., Mozer, F.S., 1985. Classification of auroral electrostatic shocks by their ion and electron associations. Journal of Geophysical Research 90, 9615–9633.

Roth, I., Temerin, M., 1997. Enrichment of ^{3}He and heavy ions in impulsive solar flares. Astrophysical Journal 477, 940–957.

Saito, H., Yoshino, T., Sato, N., 1987. Narrow-banded ELF emissions over the southern polar region. Planetary and Space Science 35, 745–752.

Sharp, R.D., Johnson, R.G., Shelley, E.G., 1977. Observation of an ionospheric acceleration mechanism producing energetic (keV) ions primarily normal to the geomagnetic field direction. Journal of Geophysical Research 82, 3324–3328.

Strangeway, R.J., Kepko, L., Elphic, R.C., Carlson, C.W., Ergun, R.E., McFadden, J.P., Peria, W.J., Delory, G.T., Chaston, C.C., Temerin, M., Cattell, C.A., Möbius, E., Kistler, L.M., Klumpar, D.M., Peterson, W.K., Shelley, E.G., Pfaff, R.F., 1998. FAST observations of VLF waves in the auroral zone: evidence of very low plasma densities. Geophysical Research Letters 25, 2065–2068.

Temerin, M., Boehm, M.H., Mozer, F.S., 1981. Paired electrostatic shocks. Geophysical Research Letters 8, 799–802.

Temerin, M., Lysak, R.L., 1984. Electromagnetic ion cyclotron mode (ELF) waves generated by auroral electron precipitation. Journal of Geophysical Research 89, 2849–2859.

Temerin, M., Roth, I., 1992. The production of ^{3}He and heavy ion enrichments in ^{3}He-rich flares by electromagnetic hydrogen cyclotron waves. Astrophysical Journal 391, L105–108.

Vaivads, A., André, M., Norqvist, P., Oscarsson, T., Rönnmark, K., Blomberg, L., Clemmons, J.H., Santolík, O., 1999. Energy transport during O^+ energization by ELF waves observed by the Freja satellite. Journal of Geophysical Research 104, 2563–2572.

Wahlund, J.-E., Eriksson, A.I., Holback, B., Boehm, M.H., Bonnell, J., Kintner, P.M., Seyler, C.E., Clemmons, J.H., Eliasson, L., Knudsen, D.J., Norqvist, P., Zanetti, L.J., 1998. Broadband ELF plasma emission during auroral energization 1. Slow ion acoustic waves. Journal of Geophysical Research 103, 4343–4375.

Whalen, B.A., Bernstein, W., Daly, P.W., 1978. Low altitude acceleration of ionospheric ions. Geophysical Research Letters 5, 55–58.

Yau, A.W., Whalen, B.A., McNamara, A.G., Kellogg, P.J., Bernstein, W., 1983. Particle and wave observations of low-altitude ionospheric ion acceleration events. Journal of Geophysical Research 88, 341–355.

Yau, A.W., Beckwith, P.H., Peterson, W.K., Shelley, E.G., 1985. Long-term (solar cycle) and seasonal variations of upflowing ionospheric ion events at DE 1 altitudes. Journal of Geophysical Research 90, 6395–6407.